Van Hove tuning of AV_3Sb_5 kagome metals under pressure and strain

Armando Consiglio,[1,*] Tilman Schwemmer,[1] Xianxin Wu,[2,3] Werner Hanke,[1] Titus Neupert,[4] Ronny Thomale,[1,5] Giorgio Sangiovanni,[1] and Domenico Di Sante[6,7]

[1]*Institut für Theoretische Physik und Astrophysik and Würzburg-Dresden Cluster of Excellence ct.qmat, Universität Würzburg, 97074 Würzburg, Germany*

[2]*Max-Planck-Institut für Festkörperforschung, Heisenbergstrasse 1, D-70569 Stuttgart, Germany*

[3]*CAS Key Laboratory of Theoretical Physics, Institute of Theoretical Physics, Chinese Academy of Sciences, Beijing 100190, China*

[4]*Department of Physics, University of Zurich, Winterthurerstrasse 190, 8057 Zurich, Switzerland*

[5]*Department of Physics and Quantum Centers in Diamond and Emerging Materials (QuCenDiEM) group, Indian Institute of Technology Madras, Chennai 600036, India*

[6]*Department of Physics and Astronomy, Alma Mater Studiorum, University of Bologna, 40127 Bologna, Italy*

[7]*Center for Computational Quantum Physics, Flatiron Institute, 162 5th Avenue, New York, New York 10010, USA*

(Received 24 November 2021; revised 18 March 2022; accepted 18 April 2022; published 26 April 2022)

From first-principles calculations, we investigate the structural and electronic properties of the kagome metals AV_3Sb_5 (A = Cs, K, Rb) under isotropic and anisotropic pressure. Charge-ordering patterns are found to be unanimously suppressed, while there is a significant rearrangement of p-type and m-type Van Hove point energies with respect to the Fermi level. Already for moderate tensile strain along the V plane and compressive strain normal to the V layer, we find that a Van Hove point can be shifted to the Fermi energy. Such a mechanism provides an invaluable tuning knob to alter the correlation profile in the kagome metal, and suggests itself for further experimental investigation. It might allow us to reconcile possible multidome superconductivity in kagome metals not only from phonons but also from the viewpoint of unconventional pairing.

DOI: 10.1103/PhysRevB.105.165146

The recently discovered family of nonmagnetic quasi-2D AV_3Sb_5 (A = Cs, K, Rb) kagome metals [1,2] represents an excellent example of compounds that allow us to study charge ordering [3–13], superconductivity [14–20], and electronic correlations [21], together with Dirac band crossing, $\mathbb{Z}_2$ nontrivial topological bands [22], chiral symmetry breaking [23], and flat-band physics [16,24].

Crystallized in the $P6/mmm$ space group, the compounds are based on a layer of vanadium atoms arranged in a kagome lattice and coordinated by antimony atoms which are organized in two sublattices. One Sb sublattice exhibits a graphitelike structure sandwiching the V kagome layer, while the other sublattice is formed by a single Sb atom centered inside the kagome hexagon.

In a kagome lattice, there are three sublattice sites per unit cell, giving rise to three electronic bands of which two are dispersive featuring a saddle point, i.e., Van Hove singularity (vHs) at $\boldsymbol{M}$, while the remaining one is exactly flat, assuming only nearest-neighbor hybridization. Interestingly, at the $\boldsymbol{M}$ points, the nesting momenta are commensurate and half the length of a reciprocal lattice vector. This leads to a 2×2 enlarged unit cell in real space for translation symmetry breaking order. Recently, the different sublattice structures of the vHs for the kagome lattice have been investigated [25]. The vHs of the upper dispersive kagome band is formed by eigenstates that feature only the contribution from one single sublattice site (p type), contrary to the lower vHs where the eigenstates distribute over two sublattices (m type) [26,27]. The p-type versus m-type property of the vHs gives rise to different types of instabilities and highlights the relevance of the substructure of a given vHs along with its proximity to the Fermi level E_F.

In this paper, we intend to investigate the Van Hove fermiology profile of kagome metals as a function of pressure and strain. In AV_3Sb_5, the correlated phases that are experimentally observed depend not only on the thickness and temperature of the material but also on the applied external stress [6,28]. In particular, a departure from ambient pressure not only unfolds a superconducting dome descending from a charge density order parent state, but also yields a second dome feature of superconductivity for increasing pressure [29–33]. The possibility of tuning interactions and competition of phases using a thermodynamic quantitylike pressure, rather than the more invasive introduction of chemical impurities, is indeed a powerful way to modify the fermiology of a material. In the process of increasing pressure values, the distance among atoms is also modified, resulting in shorter chemical bonds and different electronic structures. We demonstrate how pressure and, in particular, nonhydrostatic stresses [34], lead to interesting effects in kagome AV_3Sb_5, which may ultimately enhance the superconducting pairing strength.

Previous studies concerning structural instabilities in the AV_3Sb_5 compounds revealed the appearance of a 2×2 superlattice modulation [3,35]. It has also been pointed out that the inverse Star of David (ISD) deformation is favored

*armando.consiglio@physik.uni-wuerzburg.de

by a 2×2 charge density wave (CDW) in all three cases (A = Cs, K, Rb) [36], being locally stable and reducing the total energy with respect to the pristine phase. The same considerations also apply for the Star of David (SD) configuration, which is, however, less energetically favorable than the ISD one (see Supplemental Material [37]). Experiments have already started to explore the modification of the CDW order as a function of pressure [38,39] or the nature of the CDW itself [40]. First experiments also revealed the competition between CDW and superconductivity through uniaxial strain [18].

Starting from the ISD phase [Fig. 1(a)], we gradually increased the applied external pressure monitoring the evolution of the orbital resolved Vanadium d-states close to E_F (Fig. 2), as well as the bond lengths inside the vanadium network [Figs. 1(c)–1(e)]. The CDW phase indeed tends to noticeably reduce or suppress vHs and the density of states (DOS) in general at E_F, because CDW instabilities are related with softening of phonon modes and Fermi surface nesting [41]. Regarding the softening of phonon modes, in the Supplemental Material [37] (Appendix D) we show that the amplitude of the structural instability, signaled by imaginary phonon frequencies, reduces upon increasing pressure. We indeed find a rapid suppression of the ISD phase, reaching the pristine 1×1 phase after a certain threshold, depending on the choice of the cation A. The lowest threshold value has been obtained for the KV_3Sb_5 kagome metal [Fig. 1(e)], possibly due to the shortest interlayer distance among all considered compounds (see also Table I in Ref. [37]).

The evolution of the DOS as a function of pressure is shown in Fig. 2 for the case of CsV_3Sb_5. While the qualitative overall distribution is only weakly dependent on pressure, a closer inspection of the low-energy region around E_F reveals an orbital-dependent behavior (see Fig. 2); the coexistence of CDW and superconductivity phases for small-enough pressures can be attributed to this orbital dependence. For $P =$ 0.5 GPa, the spectral weight with vanadium d_{z^2} and $d_{x^2-y^2}$ characters is vanishing while the d_{xz} one remains finite. However, this scenario changes starting from $P = 3.0$ GPa, with the vanadium d_{z^2} and $d_{x^2-y^2}$ characters becoming non-negligible at E_F. The cases A = K, Rb follow the same trend of the V–V bond lengths shown in Fig. 1, with the ISD-pristine transition taking place for smaller pressure values (see also Supplemental Material [37]).

One of the most evident features upon increasing pressure is the strong compressive anisotropy, with the c-lattice parameter that tends to shrink faster than the a-lattice one, as a function of pressure (see Fig. 3 for the specific case of CsV_3Sb_5). Also, while the c-lattice constant exhibits a highly nonlinear behavior, the a-lattice constant is almost linear. The physical reason for this behavior relies on to the different strengths and responses to external strains of the covalent bonds along the in-plane (within the kagome networks) and out-of-plane (mostly involving V and Sb atoms) axes, respectively. The compression-isotropic scenario observed for relatively high pressure values is given by a reduced directional bonding. This is accompanied by a gradual formation of V_3Sb_5's three-dimensional structures through bonding between the V_3Sb_5 slabs, intuitively leading to an increased dispersion along the c axis. Pressure also leads to the formation of Sb_2-Sb_2 bonds. Finally, in agreement with experimental findings [31], we find that the c/a ratio exhibits a change of slope for $P \approx 8$ GPa. This is worth noting because

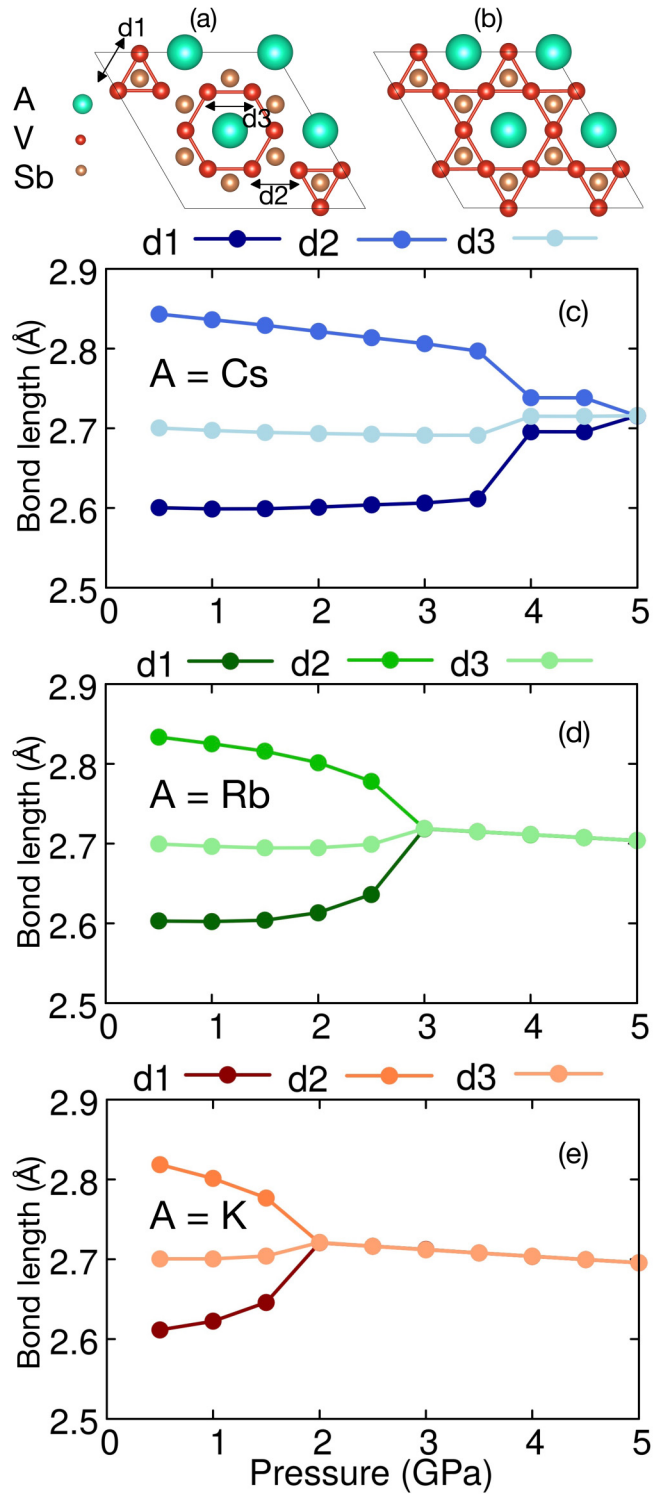

FIG. 1. Examples of ISD phase [$P = 0.5$ GPa, (a)] and pristine phase [$P \approx 4$ GPa, (b)] for the AV_3Sb_5 (A = Cs, K, Rb) kagome metals. (c) CsV_3Sb_5. (d) RbV_3Sb_5. (e) KV_3Sb_5. *d1* is the V-V distance inside the triangles, *d2* is the nearest V-V distance between the edge of a triangle and the edge of an hexagon, and *d3* is the nearest V-V distance inside the hexagons.

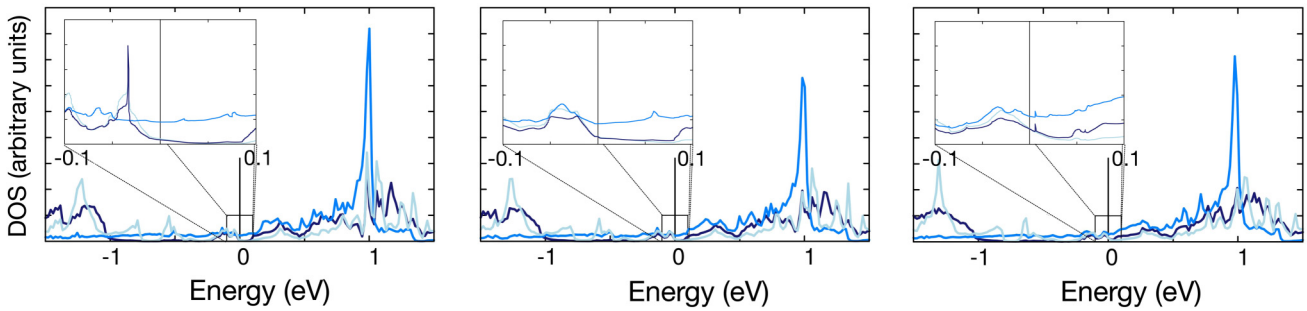

FIG. 2. Orbital resolved DOS for vanadium d orbitals in the ISD configuration of CsV_3Sb_5 at pressures $P = 0.5$ (left), 1.5 (center), and 3.0 (right) GPa.

it allows us to distinguish the low- and high-pressure regimes, but also because Lifshitz transitions can be associated to an anomaly in the c/a ratio [42].

Focusing now on the electronic band structure of AV_3Sb_5, the antimony p_z orbitals contribute primarily around the Γ point, while the Fermi surface close to $\boldsymbol{M}$ is mainly due to the vanadium d orbitals (see Supplemental Material, Appendix F). For all compounds, the general trend as a function of applied pressure, when this is high enough, is a decrease of the DOS due to the reduced interatomic distances, an obvious consequence of the increase of the bandwidth. From Fig. 4, it can be noted how the saddle points at $\boldsymbol{M}$ in proximity to E_F tend to be pushed downward, away from E_F, upon increasing the pressure. A similar scenario (not shown) holds for $k_z = \pi/c$ as both vHs's tend to be moved away from E_F, with the difference that now one vHs is above and the other below E_F. The p_z projected bands experience the most visible changes with pressure, as seen in Fig. 4, and cross the Fermi level for $P \approx 7.5$ GPa. On the contrary, the Sb p_x and p_y bands exhibit a much weaker modification besides the aforementioned bandwidth broadening. Finally, the energy position of the two vHs's for $A = \mathrm{Cs}$ is reversed with respect to $A = \mathrm{K}$, Rb. Since the two vHs's have different d-orbital characters, one can expect different Fermi surface properties, such as nesting features, for the CsV_3Sb_5 compound compared with the RbV_3Sb_5 and KV_3Sb_5 ones [26].

Besides hydrostatic pressure, the electronic properties of materials can be tuned via an applied nonhydrostatic strain (compressive or tensile) [43,44]. An efficient method for applying a strain, for example, consists of growing the material on substrates with properly chosen in-plane lattice parameters. The difference (and advantage in some cases) of doing so compared with hydrostatic pressure is that, depending on the specific bulk modulus, it is possible to shrink some chemical bonds while increasing others. For the AV_3Sb_5 family, a tensile (compressive) strain along a and b tends to increase (decrease) the in-plane spacing among vanadium atoms, and at the same time reduce (increase) the distance between the out-of-plane antimony atoms in the unit cell.

Figure 5 shows the impact of uniaxial strain on the electronic properties of AV_3Sb_5. The main outcome of this analysis is represented by the vHs evolution: uniaxial tensile strain along a is extremely effective in pushing the vHs closer to E_F. This is different from the effect of hydrostatic pressure described before. The relevance of our theoretical finding derives from recent experimental works which have reported the possibility of applying uniaxial pressures of up to ∼1 GPa, making use of a piezoelectric apparatus [45]. This, in our case, would correspond to a uniaxial distortion along a of ∼ 1%. In the Supplemental Material [37], we show that in-plane biaxial tensile strain, as well as uniaxial compressive strain along c, are likewise efficient means to tune a certain vHs closer to E_F.

To better disentangle the different contributions to the final result upon distorting the in-plane lattice parameters, we have kept the c axis fixed. In a real experiment, the in-plane elongation of the lattice parameters leads to a concomitant

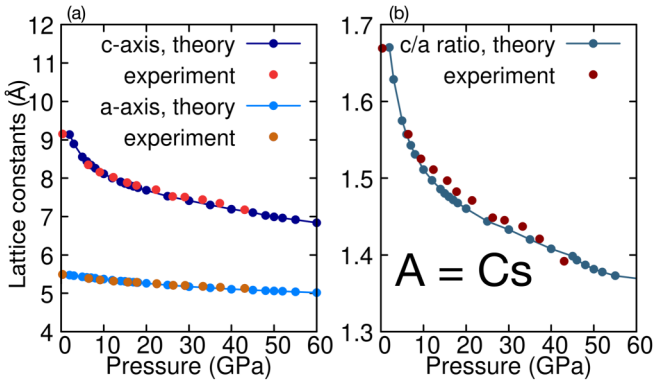

FIG. 3. Left panel: a and c lattice constants as a function of pressure for CsV_3Sb_5. Right panel: c/a ratio as a function of pressure; note the slight change of slope for $P \simeq 45$ GPa. The experimental data in both panels are taken from Ref. [31].

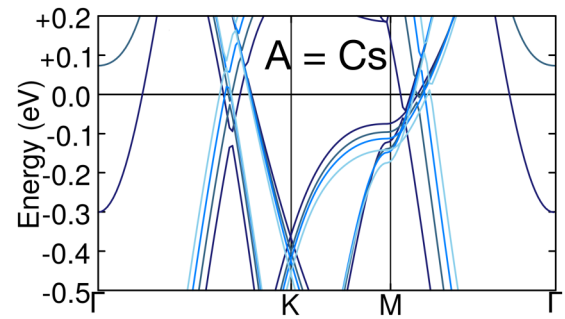

FIG. 4. Evolution of electronic band structures as a function of pressure in the proximity of the Fermi level. The fading of colors, from darker to lighter tones, corresponds to a pressure increasing. Plotted bands are for $P = 3$ GPa, 10 GPa, 15 GPa, and 20 GPa.

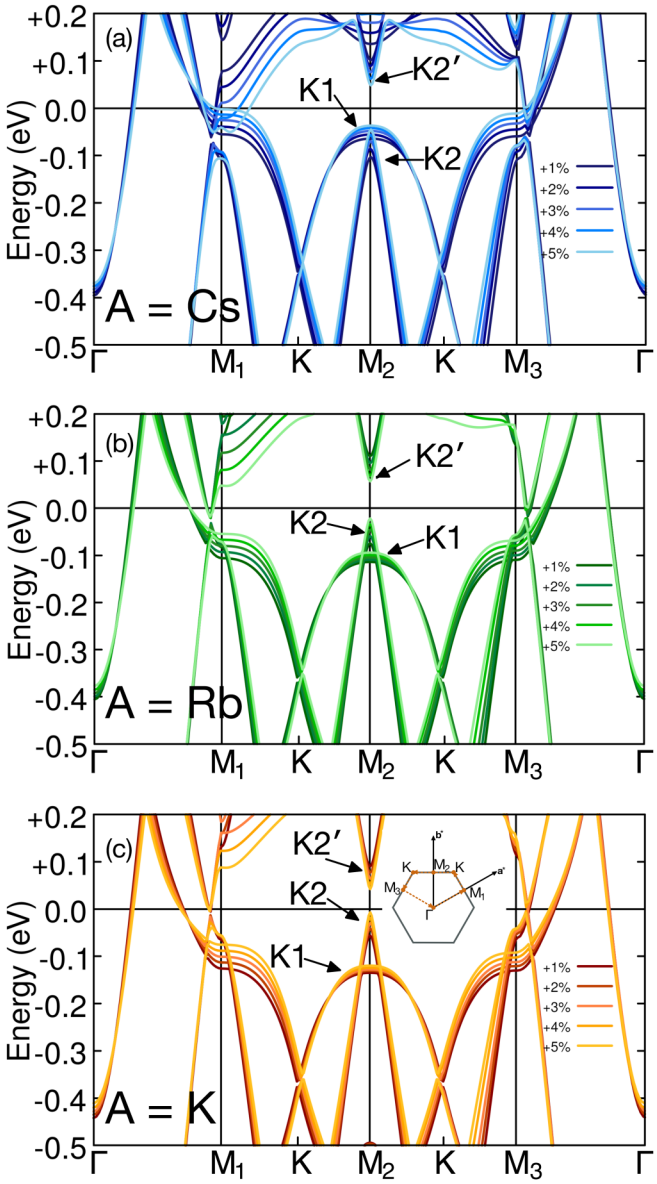

FIG. 5. Evolution of electronic band structures as a function of the uni-axial tensile strain along a-axis. Given the unstrained in-plane lattice vectors $\mathbf{a} = a(1, 0)$ and $\mathbf{b} = a(-0.5, \sqrt{3}/2)$, the $\boldsymbol{M}$ points from left to right are (0.5, 0.0), (0.0, 0.5) and (−0.5, 0.5). The percentage numbers in the legend refer to the increase of a-axis. Note that these results have been obtained while keeping fixed the c-axis for all tensile and compressive strain values. Also note that at the $\boldsymbol{M}$ points, for A = Cs, the order in energy of the K1 and K2 vHs is reversed compared to the cases A = K, Rb. The notation used is the same as in [26].

negative relaxation of the out-of-plane lattice constant. In a first approximation justified under small external stress, this is naively understood from the conservation of the unit-cell volume. It means that, concerning the evolution of the electronic properties, one must take into account the combined effect of in-plane tensile strain and the connected compressive strain along c. As a result, the vHs will likely move closer to E_F at experimentally accessible strain values.

Conclusions. Motivated by recent studies and results on the AV_3Sb_5 kagome metal compounds, we employed *ab initio* methods to monitor the evolution of the electronic and structural properties of this class of materials under a wide range of pressure values, both hydrostatic and nonisotropic. Starting from the ISD and SD charge-ordered phases, in line with previous theoretical studies [40,46], we observe for all three compounds (A = Cs, K, Rb) a suppression of the CDW already beyond a comparatively low pressure threshold ($P \approx 0.5 - 2.5$ GPa), also due to the anisotropic compression of the crystal structures. Upon higher hydrostatic pressure values ($P > 5$ GPa), we observe a change around E_F of the Sb p_z electronic bands, leading to the disappearance of the pocket at the Γ point. With regard to the vanadium d bands, which mainly contribute at the $\boldsymbol{M}$ points (see Appendix F, Supplemental Material), we find an increase of the overall bandwidth accompanied by a gradual shift of the saddle points away from E_F. In contrast, by applying uni- and biaxial deformations, it is possible to efficiently move a vHs level in the opposite direction, i.e., closer to E_F. This is particularly evident upon considering compressive strain along the c axis and/or tensile strain in the a-b plane of vanadium atoms. The distance between antimony atoms and the kagome net along c hence assumes a primary role. As a consequence of a pressure-induced vHs shift closer to E_F, even from a viewpoint of unconventional pairing, the propensity for superconductivity could increase as a function of pressure. We therefore propose strain engineering as a preeminently suited tool to optimize the superconducting transition temperature in kagome metals. In Ref. [18], an increase of T_c upon uniaxial compression along the c axis has been experimentally reported and attributed to the suppression of the CDW. In our analysis, we complement this line of reasoning by emphasizing the pressure-induced relative energy shift of the vHs (see Fig. 5 and Supplemental Material [37]), which is strongly affected by both in-plane and out-of-plane uniaxial strain. Pressure-induced effects on T_c in kagome metals can, in principle, result both from phonons and concomitant structural transitions, as well as from unconventional pairing due to Van Hove tuning. Which one turns out to be the dominant effect has to be individually analyzed experimentally.

Acknowledgments. The density functional theory work was supported by the Deutsche Forschungsgemeinschaft (DFG, German Research Foundation) through Project-ID No. 258499086-SFB 1170 and by the Würzburg-Dresden Cluster of Excellence on Complexity and Topology in Quantum Matter-ct.qmat Project-ID No. 390858490-EXC 2147. The research leading to these results has received funding from the European Union's Horizon 2020 research and innovation program under the Marie Skłodowska-Curie Grant Agreement No. 897276. This project has received funding from the European Research Council (ERC) under the European Union's Horizon 2020 research and innovation program (No. ERC-StG-Neupert-757867-PARATOP). T.N., R.T., and G.S. acknowledge support from the Deutsche Forschungsgemeinschaft (DFG, German Research Foundation) through FOR5249-449872909 (Projects No. P3 and No. P5). The authors acknowledge the Gauss Centre for Supercomputing e.V. for providing computing time on the GCS Supercomputer SuperMUC-NG at Leibniz Supercomputing Centre. The Flatiron Institute is a division of the Simons Foundation.

[1] B. R. Ortiz, L. C. Gomes, J. R. Morey, M. Winiarski, M. Bordelon, J. S. Mangum, I. W. H. Oswald, J. A. Rodriguez-Rivera, J. R. Neilson, S. D. Wilson, E. Ertekin, T. M. McQueen, and E. S. Toberer, New kagome prototype materials: Discovery of KV_3Sb_5, RbV_3Sb_5, and CsV_3Sb_5, Phys. Rev. Materials **3**, 094407 (2019).

[2] B. R. Ortiz, S. M. L. Teicher, Y. Hu, J. L. Zuo, P. M. Sarte, E. C. Schueller, A. M. Milinda Abeykoon, M. J. Krogstad, S. Rosenkranz, R. Osborn, R. Seshadri, L. Balents, J. He, and S. D. Wilson, CsV_3Sb_5: A $\mathbb{Z}_2$ Topological Kagome Metal with a Superconducting Ground State, Phys. Rev. Lett. **125**, 247002 (2020).

[3] Y. Jiang, J.-X. Yin, M. M. Denner, N. Shumiya, B. R. Ortiz, G. Xu, Z. Guguchia, J. He, Md. Shafayat Hossain, X. Liu, J. P. C. Ruff, L. Kautzsch, S. S. Zhang, G. Chang, I. Belopolski, Q. Zhang, T. A. Cochran, D. Multer, M. Litskevich, Z. Chéng *et al.*, Unconventional chiral charge order in kagome superconductor KV_3Sb_5, Nat. Mater. **20**, 1353 (2021).

[4] W.-S. Wang, Z.-Z. Li, Y.-Y. Xiang, and Q.-H. Wang, Competing electronic orders on kagome lattices at Van Hove filling, Phys. Rev. B **87**, 115135 (2013).

[5] M. L. Kiesel, C. Platt, and R. Thomale, Unconventional Fermi Surface Instabilities in the Kagome Hubbard Model, Phys. Rev. Lett. **110**, 126405 (2013).

[6] Y. Song, T. Ying, X. Chen, X. Han, X. Wu, A. P. Schnyder, Y. Huang, Jian-gang Guo, and X. Chen, Competition of Superconductivity and Charge Density Wave in Selective Oxidized $_3sb_5CsV_3Sb_5$ Thin Flakes, Phys. Rev. Lett. **127**, 237001 (2021).

[7] N. Ratcliff, L. Hallett, B. R. Ortiz, S. D. Wilson, and J. W. Harter, Coherent phonon spectroscopy and interlayer modulation of charge density wave order in the kagome metal $Cs_{V3}Sb_5$, Phys. Rev. Materials **5**, L111801 (2021).

[8] M. M. Denner, R. Thomale, and T. Neupert, Analysis of Charge Order in the Kagome Metal AV_3Sb_5 ($A = $ K, Rb, Cs), Phys. Rev. Lett. **127**, 217601 (2021).

[9] E. Uykur, B. R. Ortiz, S. D. Wilson, M. Dressel, and A. A. Tsirlin, Optical detection of the density-wave instability in the kagome metal KV_3Sb_5, npj Quantum Mater. **7**, 16 (2022).

[10] K. Nakayama, Y. Li, T. Kato, M. Liu, Z. Wang, T. Takahashi, Y. Yao, and T. Sato, Multiple energy scales and anisotropic energy gap in the charge-density-wave phase of the kagome superconductor CsV_3Sb_5, Phys. Rev. B **104**, L161112 (2021).

[11] R. Lou, A. Fedorov, Q. Yin, A. Kuibarov, Z. Tu, C. Gong, E. F. Schwier, B. Büchner, H. Lei, and S. Borisenko, Charge-Density-Wave-Induced Peak-Dip-Hump Structure and the Multiband Superconductivity in a Kagome Superconductor CsV_3Sb_5, Phys. Rev. Lett. **128**, 036402 (2022).

[12] T. Park, M. Ye, and L. Balents, Electronic instabilities of kagome metals: Saddle points and Landau theory, Phys. Rev. B **104**, 035142 (2021).

[13] C. Mielke III, D. Das, J.-X. Yin, H. Liu, R. Gupta, Y.-X. Jiang, M. Medarde, X. Wu, H. C. Lei, J. Chang, Pengcheng Dai, Q. Si, H. Miao, R. Thomale, T. Neupert, Y. Shi, R. Khasanov, M. Z. Hasan, H. Luetkens, and Z. Guguchia, Time-reversal symmetry-breaking charge order in a kagome superconductor, Nature (London) **602**, 245 (2022).

[14] M. L. Kiesel and R. Thomale, Sublattice interference in the Kagome Hubbard model, Phys. Rev. B **86**, 121105(R) (2012).

[15] Wing-Ho Ko, P. A. Lee, and X.-G. Wen, Doped kagome system as exotic superconductor, Phys. Rev. B **79**, 214502 (2009).

[16] B. R. Ortiz, P. M. Sarte, E. M. Kenney, M. J. Graf, S. M. L. Teicher, R. Seshadri, and S. D. Wilson, Superconductivity in the $\mathbb{Z}_2$ kagome metal KV_3Sb_5, Phys. Rev. Materials **5**, 034801 (2021).

[17] T. Wang, A. Yu, H. Zhang, Y. Liu, W. Li, W. Peng, Zengfeng Di, D. Jiang, and G. Mu, Enhancement of the superconductivity and quantum metallic state in the thin film of superconducting kagome metal KV_3Sb_5, arXiv:2105.07732.

[18] T. Qian, M. H. Christensen, C. Hu, Amartyajyoti Saha, B. M. Andersen, R. M. Fernandes, T. Birol, and N. Ni, Revealing the competition between charge density wave and superconductivity in CsV_3Sb_5 through uniaxial strain, Phys. Rev. B **104**, 144506 (2021).

[19] Y.-P. Lin and R. M. Nandkishore, Kagome superconductors from pomeranchuk fluctuations in charge density wave metals, arXiv:2107.09050.

[20] H. D. Scammell, J. Ingham, T. Li, and O. P. Sushkov, Chiral excitonic order, quantum anomalous Hall effect, and superconductivity from twofold Van Hove singularities in kagome metals, arXiv:2201.02643.

[21] Jianzhou Zhao, W. Wu, Y. Wang, and S. A. Yang, Electronic correlations in the normal state of the kagome superconductor KV_3Sb_5, Phys. Rev. B **103**, L241117 (2021).

[22] C. Setty, H. Hu, L. Chen, and Q. Si, Electron correlations and T-breaking density wave order in a $\mathbb{Z}_2$ kagome metal, arXiv:2105.15204.

[23] R. Ciola, K. Pongsangangan, R. Thomale, and L. Fritz, Chiral symmetry breaking through spontaneous dimerization in kagomé metals, Phys. Rev. B **104**, 245138 (2021).

[24] L. Ye, S. Fang, Min Gu Kang, J. Kaufmann, Y. Lee, J. Denlinger, C. Jozwiak, A. Bostwick, E. Rotenberg, E. Kaxiras, D. C. Bell, O. Janson, R. Comin, and J. G. Checkelsky, A flat band-induced correlated kagome metal, arXiv:2106.10824.

[25] X. Wu, T. Schwemmer, T. Müller, A. Consiglio, G. Sangiovanni, D. Di Sante, Y. Iqbal, W. Hanke, A. P. Schnyder, M. M. Denner, M. H. Fischer, T. Neupert, and R. Thomale, Nature of Unconventional Pairing in the Kagome Superconductors AV_3Sb_5 ($A = $ K, Rb, Cs), Phys. Rev. Lett. **127**, 177001 (2021).

[26] M. Kang, S. Fang, J.-K. Kim, B. Ortiz, S. H. Ryu, J. Kim, J. Yoo, G. Sangiovanni, D. Sante, B.-G. Park, C. Jozwiak, A. Bostwick, E. Rotenberg, E. Kaxiras, S. Wilson, J.-H. Park, and R. Comin, Twofold Van Hove singularity and origin of charge order in topological kagome superconductor CsV_3Sb_5, Nat. Phys. **18**, 301 (2022).

[27] Y. Hu, X. Wu, B. R. Ortiz, S. Ju, X. Han, J. Z. Ma, N. C. Plumb, M. Radovic, R. Thomale, S. D. Wilson, A. P. Schnyder, and M. Shi, Rich nature of Van Hove singularities in kagome superconductor CsV_3Sb_5, Nat Commun **13**, 2220 (2022).

[28] F. Du, Shuaishuai Luo, B. R. Ortiz, Y. Chen, W. Duan, D. Zhang, X. Lu, S. D. Wilson, Y. Song, and H. Yuan, Pressure-induced double superconducting domes and charge instability in the kagome metal KV_3Sb_5, Phys. Rev. B **103**, L220504 (2021).

[29] C. C. Zhao, L. S. Wang, W. Xia, Q. W. Yin, J. M. Ni, Y. Y. Huang, C. P. Tu, Z. C. Tao, Z. J. Tu, C. S. Gong, H. C. Lei, Y. F. Guo, X. F. Yang, and S. Y. Li, Nodal superconductivity and superconducting domes in the topological kagome metal CsV_3Sb_5, arXiv:2102.08356.

[30] K. Y. Chen, N. N. Wang, Q. W. Yin, Y. H. Gu, K. Jiang, Z. J. Tu, C. S. Gong, Y. Uwatoko, J. P. Sun, H. C. Lei, J. P. Hu, and J.-G. Cheng, Double Superconducting Dome and Triple Enhancement of T_c in the Kagome Superconductor CsV_3Sb_5 Under High Pressure, Phys. Rev. Lett. **126**, 247001 (2021).

[31] Z. Zhang, Z. Chen, Y. Zhou, Y. Yuan, S. Wang, J. Wang, H. Yang, C. An, L. Zhang, X. Zhu, Y. Zhou, X. Chen, J. Zhou, and Z. Yang, Pressure-induced reemergence of superconductivity in the topological kagome metal CsV_3Sb_5, Phys. Rev. B **103**, 224513 (2021).

[32] C. C. Zhu, X. F. Yang, W. Xia, Q. W. Yin, L. S. Wang, C. C. Zhao, D. Z. Dai, C. P. Tu, B. Q. Song, Z. C. Tao, Z. J. Tu, C. S. Gong, H. C. Lei, Y. F. Guo, and S. Y. Li, Double-dome superconductivity under pressure in the V-based kagome metals AV_3Sb_5 (A = Rb and K), Phys. Rev. B **105**, 094507 (2022).

[33] J.-F. Zhang, K. Liu, and Z.-Y. Lu, First-principles study of the double-dome superconductivity in the kagome material CsV_3Sb_5 under pressure, Phys. Rev. B **104**, 195130 (2021).

[34] A. A. Tsirlin, P. Fertey, B. R. Ortiz, B. Klis, V. Merkl, M. Dressel, S. D. Wilson, and E. Uykur, Role of Sb in the superconducting kagome metal CsV_3Sb_5 revealed by its anisotropic compression, SciPost Phys. **12**, 049 (2022).

[35] Z. Liang, X. Hou, F. Zhang, W. Ma, P. Wu, Z. Zhang, F. Yu, J.-J. Ying, K. Jiang, L. Shan, Z. Wang, and X.-H. Chen, Three-Dimensional Charge Density Wave and Surface-Dependent Vortex-Core States in a Kagome Superconductor CsV_3Sb_5, Phys. Rev. X **11**, 031026 (2021).

[36] H. Tan, Y. Liu, Z. Wang, and B. Yan, Charge Density Waves and Electronic Properties of Superconducting Kagome Metals, Phys. Rev. Lett. **127**, 046401 (2021).

[37] See Supplemental Material at http://link.aps.org/supplemental/10.1103/PhysRevB.105.165146 for additional results concerning the evolution of the electronic structure upon pressure and uni- and biaxial strain. The Supplemental Material includes Refs. [47–51].

[38] N. N. Wang, K. Y. Chen, Q. W. Yin, Y. N. N. Ma, B. Y. Pan, X. Yang, X. Y. Ji, S. L. Wu, P. F. Shan, S. X. Xu, Z. J. Tu, C. S. Gong, G. T. Liu, G. Li, Y. Uwatoko, X. L. Dong, H. C. Lei, J. P. Sun, and J.-G. Cheng, Competition between charge-density-wave and superconductivity in the kagome metal Rbv_3sb_5, Phys. Rev. Research **3**, 043018 (2021).

[39] F. H. Yu, D. H. Ma, W. Z. Zhuo, S. Q. Liu, X. K. Wen, B. Lei, J. J. Ying, and X. H. Chen, Unusual competition of superconductivity and charge-density-wave state in a compressed topological kagome metal, Nat. Commun. **12**, 3645 (2021).

[40] C. Wang, S. Liu, H. Jeon, and J.-H. Cho, Origin of charge density wave in the layered kagome metal CsV_3Sb_5, Phys. Rev. B **105**, 045135 (2022).

[41] W. Kohn, Image of the Fermi Surface in the Vibration Spectrum of a Metal, Phys. Rev. Lett. **2**, 393 (1959).

[42] S. L. Skornyakov, V. I. Anisimov, D. Vollhardt, and I. Leonov, Correlation strength, Lifshitz transition, and the emergence of a two-dimensional to three-dimensional crossover in FeSe under pressure, Phys. Rev. B **97**, 115165 (2018).

[43] W. Jiang, D. J. P. de Sousa, J.-P. Wang, and T. Low, Giant Anomalous Hall Effect Due to Double-Degenerate Quasiflat Bands, Phys. Rev. Lett. **126**, 106601 (2021).

[44] H. Huang, W. Jiang, K.-H. Jin, and F. Liu, Tunable topological semimetal states with ultraflat nodal rings in strained YN, Phys. Rev. B **98**, 045131 (2018).

[45] A. Steppke, L. Zhao, M. E. Barber, T. Scaffidi, F. Jerzembeck, H. Rosner, A. S. Gibbs, Y. Maeno, S. H. Simon, A. P. Mackenzie, and C. W. Hicks, Strong peak in T_c of Sr_2RuO_4 under uniaxial pressure, Science **355**, eaaf9398 (2017).

[46] H. LaBollita and A. S. Botana, Tuning the Van Hove singularities in AV_3Sb_5(A = K, Rb, Cs) via pressure and doping, Phys. Rev. B **104**, 205129 (2021).

[47] G. Kresse and D. Joubert, From Ultrasoft Pseudopotentials to the Projector Augmented-Wave Method, Phys. Rev. B **59**, 1758 (1999).

[48] G. Kresse and J. Furthmüller, Efficient iterative schemes for ab initio total-energy calculations using a plane-wave basis set, Phys. Rev. B **54**, 11169 (1996).

[49] J. P. Perdew, K. Burke, and M. Ernzerhof, Generalized Gradient Approximation Made Simple, Phys. Rev. Lett. **77**, 3865 (1996).

[50] V. Wang, N. Xu, J.-C. Liu, G. Tang, and W.-T. Geng, Vaspkit: A user-friendly interface facilitating high-throughput computing and analysis using VASP code, Comput. Phys. Commun. **267**, 108033 (2021).

[51] K. Momma and F. Izumi, Vesta: A three-dimensional visualization system for electronic and structural analysis, J. Appl. Crystallogr. **41**, 653 (2008).